

Aligned Carbon Nanotube Arrays Formed by Cutting a Polymer Resin–Nanotube Composite

P. M. Ajayan,* O. Stephan, C. Colliex, D. Trauth

A simple technique is described here that produces aligned arrays of carbon nanotubes. The alignment method is based on cutting thin slices (50 to 200 nanometers) of a nanotube-polymer composite. With this parallel and well-separated configuration of nanotubes it should be possible to measure individual tube properties and to demonstrate applications. The results demonstrate the nature of rheology, on nanometer scales, in composite media and flow-induced anisotropy produced by the cutting process. The fact that nanotubes do not break and are straightened after the cutting process also suggests that they have excellent mechanical properties.

Composite materials with aligned phases, which exist in a range of sizes, find many applications: for example, carbon fiber-reinforced polymer composites (1), aligned liquid crystals (2), and biocomposites (3). The aligned structures usually have high length to diameter ratios and aligning techniques range from simple manual to electrical-magnetic orientation to self-organization. As the sizes of these phases shrink to molecular dimensions (4), new properties become apparent, but control and manipulation become difficult with existing technology. Carbon nanotubes (5–8) have at-

tracted much attention because of their size and their predicted structure-sensitive properties (9–12). Although large numbers of unsorted nanotubes are available, experiments that test properties or demonstrate applications are lacking because of the problems of handling individual nanotubes and of effectively incorporating individual nanotubes into devices. Here, we demonstrate how to organize nanotubes into well-aligned arrays over micrometer scales. This could be a step toward elucidating single nanotube properties and using this material as an exploratory tool.

The rheology of fluids and viscous media has been studied in great detail in an effort to understand material flow (13). The effect of dispersion in such media and their deformation behavior allow investigation of the stresses involved during the different mechanical

processes that induce flow. Here, we demonstrate (qualitatively) the nature of the deformation process and the strength and flexibility of nanometer-sized tubes embedded in a solid, thin-film matrix during mechanical deformation of the matrix induced by cutting.

Multishell carbon nanotubes-nanoparticles prepared by the arc-discharge method (6) and purified nanotube samples (14) were dispersed randomly in a liquid epoxide-base resin by the mechanical mixing of samples (pristine samples and samples sonicated in ethanol) in the resin with a glass rod. The resin is prepared by mixing the epoxy resin (Epon-812 supplied by Shell Chemical Company; 18.2 ml), curing agents dodecenylsuccinic anhydride (DDSA; 12.4 ml) and methyl nadic anhydride (MNA; 9.4 ml), and an accelerating agent [2,4,6-tris(dimethylaminomethyl)-phenol (DMP 30); 0.7 ml] by magnetic stirring for about 2 hours. The nanotube-resin mixture, after evacuation to remove any trapped air bubbles, is poured into blocks of capsular shape and hardened by keeping it over 24 hours at above 60°C. Thin slices, ranging in thickness from 50 nm to 1 μm with lateral dimensions of a few millimeters, were cut from the composite block with a diamond knife and a Reichert-Jung Ultracut microtome (at room temperature). The thicknesses of the slices were determined by color under optical interference. The cutting speed was about 1 mm s^{-1} . The slices were supported on grids and observed in a Topcon 002B transmission electron microscope (TEM).

Because most embedded tubes were longer than the thickness of the films cut, one would expect that cutting would make transverse sections of tubes unless the tubes remain parallel to the cutting plane. However, the tubes could also be pulled out of the resin or deformed within a softer matrix during cutting. In fact, the above method (and resin) is routinely used to make sections of clay fibers such as crysotiles (15), quartz-based minerals, and kerogen minerals. Indeed, we see in Figs. 1 through 4 that no cross sections of nanotubes are produced.

Images of slices (<200 nm thick) show that the tubes were preferentially oriented during the cutting process. The direction of knife movement was judged from the periodic and faint oscillations in contrast seen on the matrix film, and the tubes were almost always aligned along this direction. The orienting effect was seen over the entire slice, although arrays of tubes with reasonable density existed over areas of a few square micrometers. Figure 1 shows an area with nanotubes and nanoparticles scattered in a thin section (~ 50 nm) of the resin. All the longer and thinner tubes have been oriented, whereas the thicker and shorter tubes and the nanoparticles have a random orientation. In most cases, the

P. M. Ajayan, O. Stephan, C. Colliex, Laboratoire de Physique des Solides, URA 002, Batiment 510, Université Paris-sud, Orsay 91405, France.

D. Trauth, Laboratoire de Géologie des Muséum, URA 723, 43 Rue Buffon, Paris 75005, France.

* To whom correspondence should be addressed.

aligned tubes were straightened along their entire length. Holes in the film are a result of the small film thickness and the clustering of nanoparticles.

Figure 2A shows the degree of alignment achieved for a pure nanotube sample (no nanoparticles) in a slightly thicker slice (~ 80 nm). There are very few defects (holes) in the film, and most of the longer and thinner tubes are aligned. Once again, the shorter and thicker tubes (residues of oxidation) were not oriented. We generally observed that the tubes $\sim <10$ nm in diam-

eter and longer than few hundred nanometers are aligned. Figure 2, B and C, shows local areas with arrays of well-oriented and separated tubes that have relatively uniform spacing between them. Such regions occur commonly in the slices. Comparing the lengths of nanotubes in the images from the sections and from the pristine powder samples, we find that no noticeable changes have occurred in the fiber length distribution upon cutting. When the thickness of the slices increases beyond 0.3 to 0.5 μm , the aligning effect becomes less pronounced, disappearing above 1 μm .

It is difficult to unambiguously determine if the aligned tubes are present on the surface or embedded inside the films. Some tubes present on the surface came off easily, creating one-dimensional cavities that gave strong reverse contrast during observation with electron microscopy. Most tubes remained well attached to the films (even during film expansion under electron irradiation), suggesting that they adhered to the matrix phase. The difference in focus conditions for individual tubes (Fig. 2A) also suggests the difference in relative positions (normal to the film) of the tubes within each slice. The sections here are extremely thin and should be supported on substrates (glass slides, for example) for experiments. If the matrix resin is removed by selective etching, arrays of parallel nanotubes could be exposed, which would be ideal substrate patterns for the fabrication of one-dimensional nanostructures.

From these observations, we can present a model to explain the effect, which resembles the pullout of fibers from a rigid matrix when

a fiber composite is mechanically labeled. The stress distribution in the films during cutting depends on such parameters as cutting speed, ductility, hardness of the matrix, and the mechanical properties of the dispersed tubes. The directional cutting process creates shear that induces flow of material. The aligning here is similar to the aligning of rodlike dispersions in fluids during shear flow (13). The tubes that come in contact with the knife during cutting are pulled out or are deformed from the matrix and are oriented unidirectionally on the newly formed surface. The tubes confined between the cutting plane and the air-film interface will be moved within the matrix, stretched, or deformed by shear. In the rigid resin matrix, because the lengths aligned (or pulled out) during cutting are not different from the lengths of the original fibers, one can suggest that the fibers are mechanically very strong or that the interfacial bond between tubes and the matrix is weak. In addition, the facts that breaking is not observed for the tubes and that the tubes are well straightened by the cutting process suggest excellent mechanical properties for the tubes. The separation between individual tubes observed in the sections after cutting is due to the deformation of the matrix resin that separates individual tubes. As the thickness of the section increases, the cross section over which forces are distributed also increases, decreasing the stresses and the ability to deform and align tubes.

When tubes are entangled and crowded, proper distribution is not achieved and tearing of the film was observed. A dilute distribution serves best as these tubes are not locked on each other during aligning. In

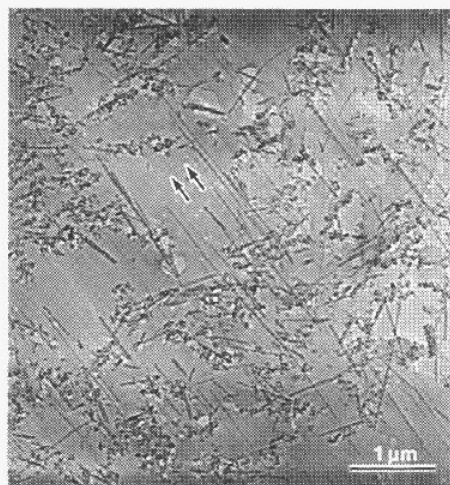


Fig. 1. Low-magnification TEM image from a slice (50 nm thick) with a distribution of nanotubes and nanoparticles (closed graphite polyhedra). Most of the long tubes have been oriented by cutting; holes in the film are due to the clustering of nanoparticles. Two parallel arrows in all figures indicate the cutting direction.

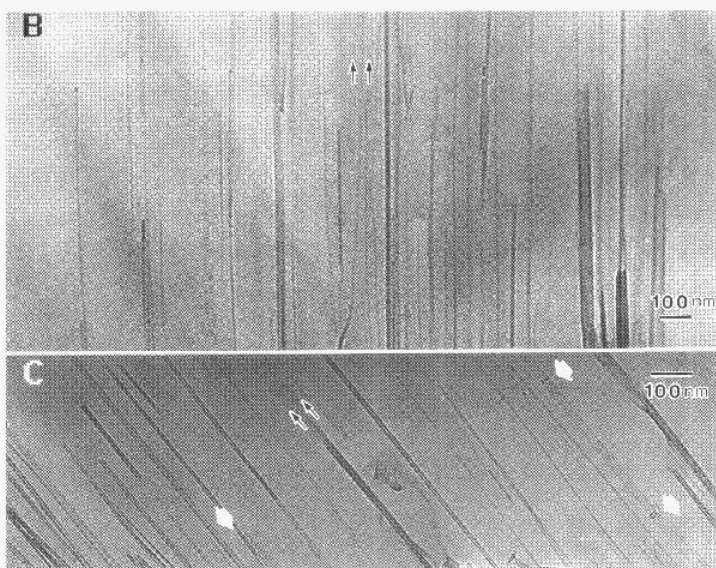
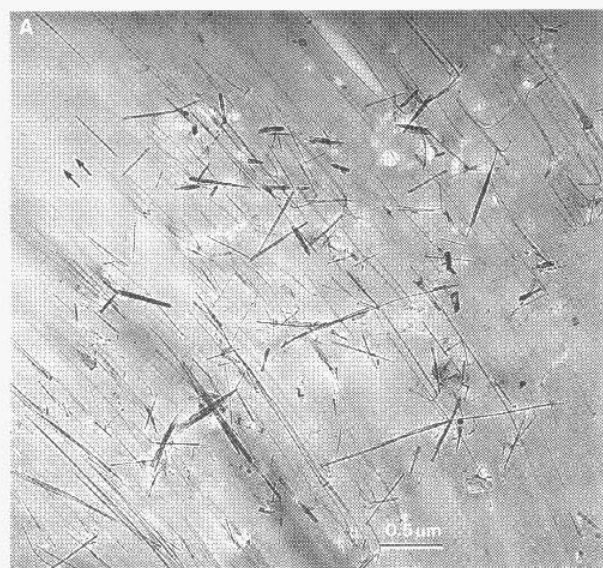


Fig. 2. (A) Low-magnification TEM image from a pure nanotube sample in a 80-nm-thick film. The alignment of the long, thin tubes is clear, but the thicker, shorter tubes remain randomly oriented. (B and C) Images at higher magnification showing local areas of films with perfectly parallel and

separated nanotube arrays. The hollow interiors of the tubes are seen clearly in (C). Arrowheads show dark lines across tube diameters, which could correspond to sharply bent basal planes (during cutting) normal to the axis.

thicker films (>100 nm), holes were rarely observed and edges showed tubes that were pulled out, with fairly good alignment in the film. Smaller tubes are extremely flexible and are easily bent and aligned segmentally (Fig. 3), as seen in dispersions of flexible chains during fluid flow (13). Our results suggest that carbon nanotubes may be used as extremely strong (along the axis), flexible (bending) nanofibers.

The deformation of nanotubes observed in the solid resin also provides information on other mechanical behaviors, such as defect forma-

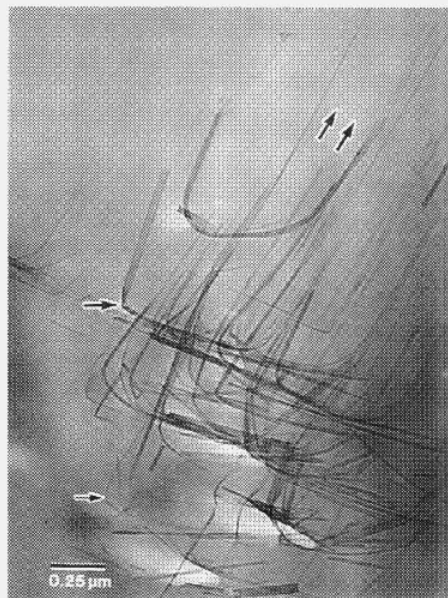
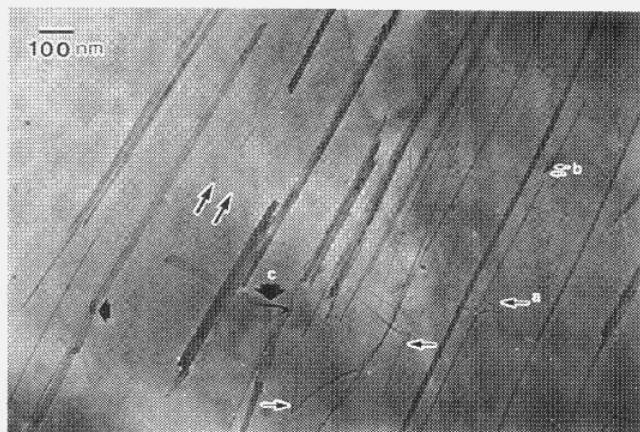


Fig. 3. Images showing the effect of the clustering of tubes on alignment. No holes are formed on a thick film (200 nm), but thinning occurs at the sites of tube clusters (lighter contrast). End segments of the tubes are aligned in the cutting direction. Arrows indicate the nature of bending; the larger tube has been twisted but the smaller one shows no such defect. The larger twisted tube has been flattened on the upper segment, as indicated by the apparent increase in the diameter or the separation between the tube walls that produce the line contrast in the images of nanotubes (5).

Fig. 4. Image from an area of the film where defects on nanotubes are concentrated. Defects marked by letters (a, b, and c) are described in the text, and similar arrows denote similar defects. The tube on which defect c is marked seems to have been flattened (compare its morphology with that of the flattened tube in Fig. 3) by cutting, but flattening of tubes is observed only in rare cases. The tubes are oriented along the cutting direction and remain straight and parallel for many micrometers.



tion and the tribological character of nanotubes. Figure 4 shows typical defects created on the tubes by deformation. These defects are usually concentrated in certain local regions (perhaps a result of uneven contact between the knife and the matrix). A commonly observed defect is kinks (marked a) of different angles that arise from bending or buckling that results from compressive stresses parallel to the basal planes. Breaking of tubes (marked b) was seen very rarely. Twisting (marked c in Fig. 4 and indicated in Fig. 3) from shear along the axis was observed in larger tubes (especially with small numbers of layers and large hollow interiors; the size of tubes that show this defect in Fig. 4 is >25 nm). Twisting deforms the cross sections into polyhedral shapes (Fig. 4). The aligning process should work very well for single-layer nanotubes (7, 8) if these tubes with their small diameters and large lengths can be isolated.

It is remarkable that few of the tubes were flattened during the cutting process (see Figs. 3 and 4). Tubular shapes seem to have a stable geometry. This observation is contrary to recent reports stating that small nanotubes could be easily flattened even by weak van der Waals forces between individual tubes (16) or by the interaction of tubes with the tip of an atomic force microscope (17). The central hollows in the tubes can be seen in the images along their entire lengths (Figs. 2C, 3, and 4); some open tubes were partially filled with the resin, which could have an effect on individual tube properties.

Thin sections of resins supporting oriented nanotubes may be compared to some liquid crystal (nematic) phases. In liquid crystals, molecular alignment is often achieved by confining the crystals between mechanically rubbed surfaces (18, 19), which seems to resemble the cutting process we have described here. The aligning method we report here relies on the basic principle of mechanical deformation and should work for fibers of any size that are mechanically strong. We are not aware of any other techniques (20) that may be used to align carbon tubes of such small

dimensions. One could imagine methods based on mechanical working [for example, extrusion and cold drawing that are used to align larger carbon and textile fibers (20)], but the amounts of pure samples usually available are very small (less than gram quantities for purified nanotubes).

The availability of aligned nanotube arrays over large areas will make it possible to measure transport properties [the average properties of nanotube bundles have been measured (21), but these measurements have failed to test the theoretical predictions on single tubes]. Measurements on single tubes, for example, using the scanning tunneling microscope, have been accomplished with some difficulty (22) (the experiments are complicated by the problem of tube orientation and dispersion). With a well-separated parallel array of exposed nanotubes (those present on the surface or after etching away the matrix resin locally), such tests can be carried out with ease by scanning from one tube to the other to compare properties that have been theoretically predicted to depend on tube size and the helicity in the hexagonal carbon network (which will vary from tube to tube). Future work should be directed toward increasing areas with aligned tubes by optimizing the starting distribution and the density of tubes in the composite mixture.

REFERENCES AND NOTES

1. M. S. Dresselhaus *et al.*, in *Graphite Fibers and Tiliaments*, M. Cardona, Ed. (Springer, Berlin, 1988).
2. C. W. Cray and P. A. Winsor, Eds., *Liquid Crystals and Plastic Crystals* (Ellis Horwood, London, 1974), vol. 2.
3. P. A. Bianconi, J. Lin, A. R. Strzelecki, *Nature* **349**, 315 (1991).
4. P. Calvert, *ibid.* **357**, 365 (1992).
5. S. Iijima, *ibid.* **354**, 56 (1991).
6. T. W. Ebbesen and P. M. Ajayan, *ibid.* **358**, 220 (1992).
7. S. Iijima and T. Ichihashi, *ibid.* **363**, 603 (1993).
8. D. S. Bethune *et al.*, *ibid.*, p. 605.
9. J. W. Mintmire, B. I. Dunlop, C. T. White, *Phys. Rev. Lett.* **68**, 631 (1992).
10. N. Hamada, S. Sawada, A. Oshiyama, *ibid.*, p. 1579.
11. M. S. Dresselhaus, *Nature* **358**, 192 (1992).
12. P. M. Ajayan and S. Iijima, *ibid.* **361**, 333 (1993).
13. H. L. Goldsmith and S. G. Mason, in *Rheology, Theory and Applications*, F. R. Eirich, Ed. (Academic Press, New York, 1967), vol. 4, pp. 86–246.
14. T. W. Ebbesen, P. M. Ajayan, H. Hiura, K. Tanigaki, *Nature* **367**, 519 (1994).
15. T. Sudo *et al.*, *Electron Micrographs of Clay Minerals* (Developments of Sedimentology Series 31, Elsevier, Amsterdam, 1981).
16. R. D. Ruoff *et al.*, *Nature* **364**, 514 (1993).
17. H. Hiura *et al.*, *ibid.* **367**, 148 (1994).
18. H. Hatton *et al.*, *Appl. Phys. Lett.* **64**, 1103 (1994).
19. P. J. Shannon, W. M. Gibbons, S. T. Sun, *Nature* **368**, 532 (1994).
20. A. P. Levill, Ed., *Whisker Technology* (Wiley-Interscience, London, 1970).
21. S. N. Song, X. K. Wang, R. P. H. Chang, J. B. Ketterson, *Phys. Rev. Lett.* **72**, 697 (1994).
22. C. H. Olk and J. P. Heremans, *J. Mater. Res.* **9**, 259 (1994).
23. P.M.A. acknowledges funding from the Grant of French Ministere des Affaires Etrangeres.

9 May 1994; accepted 5 July 1994